High-Resolution Poly(ethylene terephthalate) (PET) Hot Embossing at Low Temperature: Thermal, Mechanical, and Optical Analysis of Nanopatterned Films

ARTICLE *in* LANGMUIR · NOVEMBER 2008

Impact Factor: 4.46 · DOI: 10.1021/la801706q · Source: PubMed

6 AUTHORS, INCLUDING:

Francesca Signori
Consorzio Interuniversitario Nazionale per …
34 PUBLICATIONS **513** CITATIONS
SEE PROFILE

Pasqualantonio Pingue
Scuola Normale Superiore di Pisa
49 PUBLICATIONS **505** CITATIONS
SEE PROFILE

Simona Bronco
National Research Council (CNR, Pisa, Italy)
74 PUBLICATIONS **873** CITATIONS
SEE PROFILE

Francesco Ciardelli
Università di Pisa
345 PUBLICATIONS **4,767** CITATIONS
SEE PROFILE

Langmuir

Article

High-Resolution Poly(ethylene terephthalate) (PET) Hot Embossing at Low Temperature: Thermal, Mechanical, and Optical Analysis of Nanopatterned Films

Marco Cecchini, Francesca Signori, Pasqualantonio Pingue, Simona Bronco, Francesco Ciardelli, and Fabio Beltram

Langmuir, **2008**, 24 (21), 12581-12586 • DOI: 10.1021/la801706q • Publication Date (Web): 04 October 2008

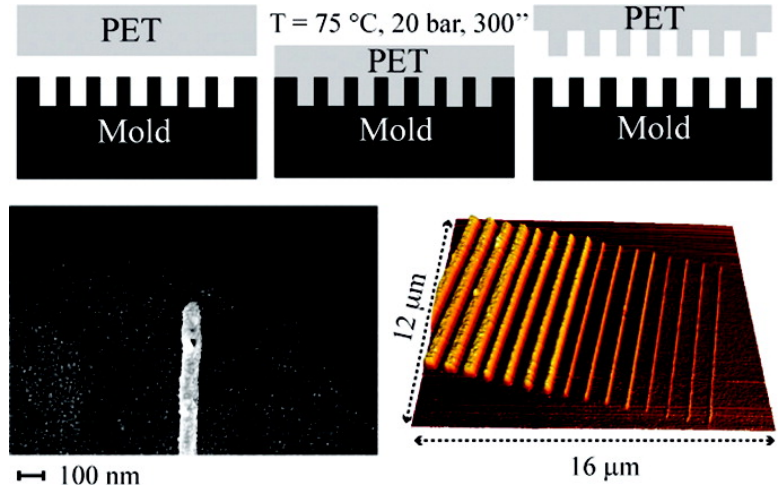

More About This Article

Additional resources and features associated with this article are available within the HTML version:

- Supporting Information
- Access to high resolution figures
- Links to articles and content related to this article
- Copyright permission to reproduce figures and/or text from this article

View the Full Text HTML

High-Resolution Poly(ethylene terephthalate) (PET) Hot Embossing at Low Temperature: Thermal, Mechanical, and Optical Analysis of Nanopatterned Films

Marco Cecchini,*[,†,‡] Francesca Signori,[§] Pasqualantonio Pingue,[‡] Simona Bronco,[§] Francesco Ciardelli,[||] and Fabio Beltram[†,‡]

Scuola Normale Superiore and Italian Institute of Technology, I-56126 Pisa, Italy, Laboratorio NEST-Scuola Normale Superiore, Piazza San Silvestro 12, I-56127 Pisa, Italy, and CNR-INFM PolyLab and Dipartimento di Chimica e Chimica Industriale, Università di Pisa, via Risorgimento 35, I-56126 Pisa, Italy

Received June 3, 2008. Revised Manuscript Received July 31, 2008

In this work we present controlled, low-damage nanotopographic surface modification of poly(ethylene terephthalate) (PET). High-resolution nanopatterning over macroscopic areas was performed by "*low-temperature*" hot embossing lithography (HEL). While for standard HEL the temperature is typically raised up to many tens of Celsius degrees above the polymer glass transition temperature (T_g), we demonstrate optimal results at a temperature very close to the bulk T_g of PET (72 °C). Nanopits and nanobarcodes were transferred onto the surface of PET commercial sheets, demonstrating reliable sub-100 nm resolution over macroscopic areas. Sample optical, mechanical, and thermal characteristics were systematically analyzed before and after embossing at low (75 °C) and high (150 °C) temperature by attenuated total reflection Fourier transform infrared (ATR-FTIR) spectroscopy, tensile tests, and differential scanning calorimetry (DSC). We show that, while conventional high-temperature HEL can lead to dramatic degradation of the polymer in terms of transparency, flexibility, and crystallinity content, our low-temperature process fully maintains original surface and bulk substrate properties.

1. Introduction

Hot-embossing (or nanoimprint) lithography (HEL) is a straightforward, low-cost, high-throughput, and high-resolution patterning technique.[1] Typically, a hard mold with a micro/nanofabricated pattern on its surface is pressed into a thermoplastic polymer prepared as a thick slice or spin-coated onto a rigid or flexible substrate. In many cases, this unconventional procedure enables controlled surface modification of plastic materials whereas standard lithographic schemes are not applicable because of the general incompatibility of plastics with the solutions (i.e., developers, organic solvents, etc.) involved in these conventional micro/nanofabrication processes. High-resolution nanopatterning of many thermoplastic polymers was demonstrated, but, to the best of our knowledge, controlled high-resolution nanopatterning of poly(ethylene terephthalate) (PET) was never achieved.

PET is a thermoplastic polymer with uncommon physical, mechanical, and chemical characteristics that make it very attractive for large-scale applications, mainly in the packaging field. Its properties include high transparency and flexibility, impact-resistance, light weight, and low gas permeability (especially to oxygen, carbon dioxide, and water vapor). PET has also optimal physicochemical characteristics for the fabrication of nanostructured artificial tissues or, owing to its flexibility and transparency, for the engineering of innovative plastic displays based on organic light-emitting devices.[2]

Exploitation of this material requires the definition of specific, high-resolution processing techniques, which allow submicrometer patterning while maintaining unchanged physicochemical characteristics of the polymer. Standard micro/nanofabrication processes are not suitable for PET. Indeed, PET reacts with several developers and absorbs UV radiation,[3] resulting in macroscopic material aging and lower mechanical performances.[4,5] Moreover, owing to its relatively low glass transition temperature (T_g in the 70−85 °C range), it cannot be heated up to typical resist baking temperatures without losing its nominal characteristics. High temperature treatments promote material reorganization at the macromolecular level, resulting in an altered amorphous/crystalline ratio content. As a consequence, material thermal behavior, optical and mechanical properties dramatically change, leading to evident loss of transparency and flexibility.

In order to take advantage of the excellent flexibility and transparency of PET foils, they were introduced as substrates for depositing metallic or monomeric/polymeric nanostructures.[6−8] Some authors exploited UV curing or thermal nanoimprint lithography (NIL) on original resins deposited onto PET, but controlled nanomodification on PET itself was still not introduced. For example, Lee et al.[7,8] demonstrated an original process by exploiting the thermal curing characteristics of a liquid-phase monomer and NIL. They could obtain arrays of lines with a lateral dimension of 100 nm.[7] Based on a UV-curing resin, a similar approach was exploited to mask the substrate for a metal evaporation and lift-off process: 100 nm metal lines (Ti/Au) were finally transferred onto PET.[8] Other nonconventional processes were also introduced, allowing the transfer of patterned 2D plastic layers and the formation of multistacked 3D nanostructures.[9]

* To whom correspondence should be addressed. E-mail: m.cecchini@sns.it.
† Scuola Normale Superiore and Italian Institute of Technology.
‡ Scuola Normale Superiore and NEST-CNR-INFM.
§ CNR-INFM PolyLab and Dipartimento di Chimica e Chimica Industriale, Università di Pisa.
|| Dipartimento di Chimica e Chimica Industriale, Università di Pisa.

(1) Schift, H. *J. Vac. Sci. Technol., B* **2008**, *36*, 458.
(2) Li, Y.; Tan, L.-W.; Hao, X.-T.; Ong, K. S.; Zhu, F.; Hung, L.-S. *Appl. Phys. Lett.* **2005**, *86*, 153508.
(3) LaFemina, J. P.; Arjavalingam, G. J. *J. Phys. Chem.* **1991**, *95*, 984.
(4) Coltro, L.; Padula, M.; Saron, E. S.; Borghetti, J.; Buratin, A. E. P. *Packag. Technol. Sci.* **2003**, *16*, 15.
(5) Wang, W.; Taniguchi, A.; Fukuhara, M.; Okada, T. *J. Appl. Polym. Sci.* **1998**, *67*, 705.
(6) Liao, W.-c.; Hsu, S. L.-C. *Nanotechnology* **2007**, *18*, 065303.
(7) Lee, H.; Hong, S.; Yang, K.; Choi, K. *Microelectron. Eng.* **2006**, *83*, 323.
(8) Lee, H.; Hong, S.; Yang, K.; Choi, K. *Appl. Phys. Lett.* **2006**, *88*, 143112.

10.1021/la801706q CCC: $40.75
Published on Web 10/04/2008

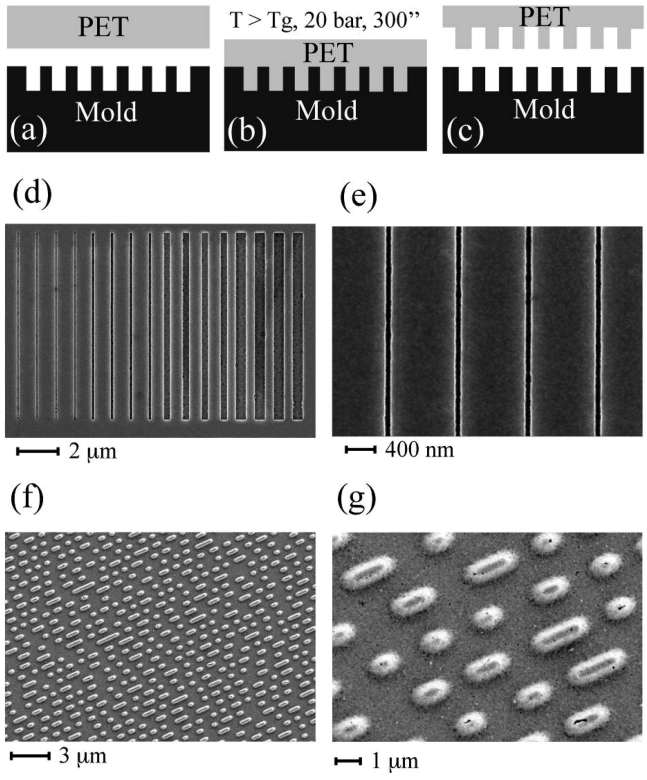

Figure 1. Fabrication process of PET nanostructures and mold characterization. (a) PET foils were placed on top of the silicon mold and softened by increasing the temperature up to 75 °C. (b) 20 bar pressure was applied for 5 min before cooling down to 50 °C. (c) The pressure was finally released, and mold and PET detached. (d,e) "Hi-res"-molds imaged by SEM: low magnification image of a nanograting (d); detail for the 60 nm wide grooves (e). (f,g) "DVD"-molds imaged by SEM: low magnification overview (f); high-resolution detail of the stamper protrusions.

Here, we demonstrate low-damage nanotopographic surface modification of PET. High-resolution nanopatterning over macroscopic areas was performed by "*low-temperature*" hot embossing lithography. We shall show DVD-like nanopits and nanobarcodes transferred on PET commercial substrates, demonstrating reliable sub-100 nm resolution while maintaining unaltered optical, mechanical, and thermal characteristics.

2. Materials and Methods

2.1. Hot Embossing Lithography (HEL). Nanopatterns were fabricated into PET substrates by HEL. We used standard imprint schemes which are based on a combination of pressure and heat to transfer patterns from a mold directly to the polymeric material (Figure 1a−c).[10]

We fabricated high-resolution molds ("hi-res"-molds) by means of electron-beam lithography (EBL) and reactive-ion etching (RIE) starting from commercial p-doped silicon wafers (SYLTRONIX, France). Each mold consists of a quarter 2′ Si wafer, initially processed by EBL to generate arrays of gratings into 250 nm thick poly(methyl methacrylate) (PMMA) film. PMMA was used successively as an etch mask during the RIE lithographic step that led to pattern transfer into the silicon substrate. After cleaning with acetone/isopropanol and oxygen plasma, the molds were characterized by scanning electron and atomic force microscopy. Figure 1d and e shows the grating geometry and a high-magnification image of the narrowest lines, respectively. Each grating consisted of grooves with different line widths, from 500 nm down to about 60 nm. The pitch and the depth were 1 μm and 80 nm, respectively. The gratings were repeated in arrays in order to cover macroscopic areas of the mold. Before embossing, the molds were silanizated [silanization solution: dimethyldichlorosilane in heptane (Fluka)] in order to obtain low-energy surfaces. This allowed proper master−replica separation after imprint, improving the fidelity and reproducibility of the process.[11]

"DVD"-molds from Obducat were used for experiments where very high resolution was not necessary. The geometry of the pattern was similar to that present on commercial DVD stampers, with typical dimensions of several hundreds of nanometers. Figure 1f and g shows low- and high-magnification scanning electron microscopy (SEM) images, respectively, of a "DVD"-mold. Specifically, "DVD"-molds were used to fabricate PET samples for thermal and optical analyses and for tensile tests.

PET foils (0.25 mm thick, Goodfellow LS305225) were embossed using an Obducat Nanoimprint 24 system. After cleaning with nitrogen blow, the PET was placed on top of the mold and softened by increasing the temperature above the film glass transition temperature (Figure 1a). The imprinting machine does not apply homogeneous heating to the bulk of the polymer, but heating is transferred to the mold and finally to the polymer film by contact heating. We should point out that, because of the low thermal conductivity of PET foils, only the film surface will be in thermal equilibrium with the mold during processing. A pressure of 20 bar was then applied for 5 min (Figure 1b) before cooling down to 50 °C (Figure 1c). Finally, the pressure was released, and the mold and PET were softly detached with a scalpel. Two sets of samples were fabricated, at two different embossing temperatures: 75 °C (named PET75) and 150 °C (named PET150).

2.2. Atomic Force and Scanning Electron Microscope Imaging. The topography of the embossed films was systematically analyzed by atomic force (AF) and scanning electron microscopy. AFM analysis was carried out in tapping mode, by using a Veeco diCaliber and high aspect ratio silicon tip. SEM images were acquired after having coated the samples with a 20 nm thick gold layer by thermal evaporation. The metal layer was shorted to the SEM sample holder to avoid electron charging during the imaging characterization. The substrates were then loaded into a LEO 1525 field emission scanning electron microscope, and image acquisition was carried out by secondary-electron detection.

2.3. Differential Scanning Calorimetry (DSC). DSC analyses were carried out by using a Perkin-Elmer DSC7 calorimeter, working in the 0−300 °C range. Samples (5−8 mg of PET packed in aluminum pans) were heated from 30 to 300 °C (first heating), cooled down to 0 °C (first cooling), and then heated again up to 300 °C (second heating). The heating and cooling rate was set at 10 °C/min in all cases. Indium and tin were used as calibration standards. T_g was taken as the inflection point of the heat capacity change.[12] The degree of crystallinity of the samples (χ) was determined according to eq 1:

$$\chi = \frac{\Delta H_m}{\Delta H_{m,0}} \tag{1}$$

where ΔH_m is the measured heat of fusion of the analyzed samples and $\Delta H_{m,0} = 135$ J/g is the heat fusion of a PET perfect crystal.[13]

2.4. Attenuated Total Reflection Fourier Transform Infrared (ATR-FTIR) Spectroscopy. ATR-FTIR spectroscopy was carried out on PET films by using two different spectrometers: a Jasco FT-IR 4100 (Ge crystal, $n = 4.0$) and a Perkin-Elmer Specrtum GX (ZnSe crystal, $n = 2.4$). Owing to the different refractive indices of the crystals, the electromagnetic radiation penetration depth into the PET films was different in the two cases.[14] For an incident angle of 45° at 1340 cm^{-1}, penetration depths were 500 nm for the Ge setup (method 1) and 2100 nm for the ZnSe setup (method 2).

(9) Han, K.-S.; Hong, S.-H.; Lee, H. *Appl. Phys. Lett.* **2007**, *91*, 123118.
(10) Chou, S. Y.; Krauss, P. R.; Renstrom, P. J. *J. Vac. Sci. Technol., B* **1996**, *14*, 4129.
(11) Beck, M.; Graczyk, M.; Maximov, I.; Sarwe, E.-L.; Ling, T. G. I.; Keil, M.; Montelius, L. *Microelectron. Eng.* **2002**, *61*, 441.
(12) Wunderlich, B. In *Thermal Characterization of Polymeric Materials*; Turi, E.A., Ed.; Academic Press: San Diego, 1997; p 380.
(13) Liangbin, L.; Rui, H.; Ling, Z.; Shiming, H. *Polymer* **2001**, *42*, 2085.
(14) Kirov, K. R.; Hazel, E. *Macromolecules* **2005**, *38*, 9258.

By following the procedure of Zhang et al.,[15] sample crystallinity was evaluated by calculating the fraction of the *trans*-EG conformer with respect to the *gauche*-EG conformer by using the following formula:

$$T = \frac{A_{1340}}{A_{1340} + (6.6 \times A_{1370})} \quad (2)$$

where A_{1340} and A_{1370} are the integrated absorbances at 1340 and 1370 cm^{-1}, attributed, respectively, to the *trans*-EG conformer and the *gauche*-EG conformer of the PET macromolecular chains. Peak integration was carried out in the 1386−1360 cm^{-1} (*trans*-EG conformer) and 1330−1355 cm^{-1} (*gauche*-EG conformer) ranges.

2.5. Tensile Tests. Tensile tests were carried out according to American Society for Testing and Materials (ASTM) D638 MIII[16] protocol, by using a Tinius Olser H10KT tensile tester equipped with a 500 N load cell. As specified by the ASTM, specimens were conditioned ($T = 20$ °C, $P = 1$ atm, $t = 48$ h, 50% relative humidity) before analysis. Measurements were carried out at a crosshead speed of 10 mm/min. Finally, tensile stress, strain, and elastic modulus were calculated by an average of the results obtained from the load elongation curves acquired for 8 to 15 specimens for each sample.

3. Results and Discussion

3.1. Nanopatterning of PET. Nanopatterns were fabricated into 0.25 mm thick PET substrates by HEL. This technique is based on sample heating and pressure application to facilitate mold cavity filling by the polymer. Typically, this kind of process requires an increase of the sample temperature up to tens of degrees over its glass transition temperature (T_g), often causing fast degradation of plastic substrates.[17,18] The bulk glass transition temperature of our unprocessed PET foils (named BARE-PET) measured by DSC analysis (see section 3.3) is $T_g = 72$ °C. Hot embossing was performed at two different temperatures: $T_h = 150$ °C and $T_l = 75$ °C. T_h is well above T_g, while T_l is just a few degrees higher. This led to very different crystallization times for the two process conditions. T_h is expected to induce significant modification of the PET crystallization state; T_l was chosen in order to have minimal impact on the film crystallinity during the process time (300 s).

HEL was first tested with "DVD"-molds in order to verify the proper transfer of patterns with noncrucial dimensions. Following standard procedures, we started by setting the process temperature to T_h, which leads to low viscosity and easy polymer flow into the mold cavities. However, rather broadened nanostructures (see AFM image in Figure 2e) were obtained and film transparency was lost. A comparison between optical microscopy images of pristine PET (Figure 2a) and Figure 2c highlights the variation of the optical properties of PET150, which changed from transparent to completely opaque, suggesting that unacceptable crystallization had occurred. Since transparency is one of the most important characteristics of PET, we must conclude that standard "high-temperature" HEL is not suitable for practical uses.

The imprint temperature was then reduced in order to test the possibility to replicate the mold with good fidelity while limiting crystallization as much as possible. To this end, the process was performed at $T_l = 75$ °C, that is, very close to PET glass transition temperature. Figure 2d displays an AFM image of PET75 and demonstrates accurate pattern transfer, with no presence of the

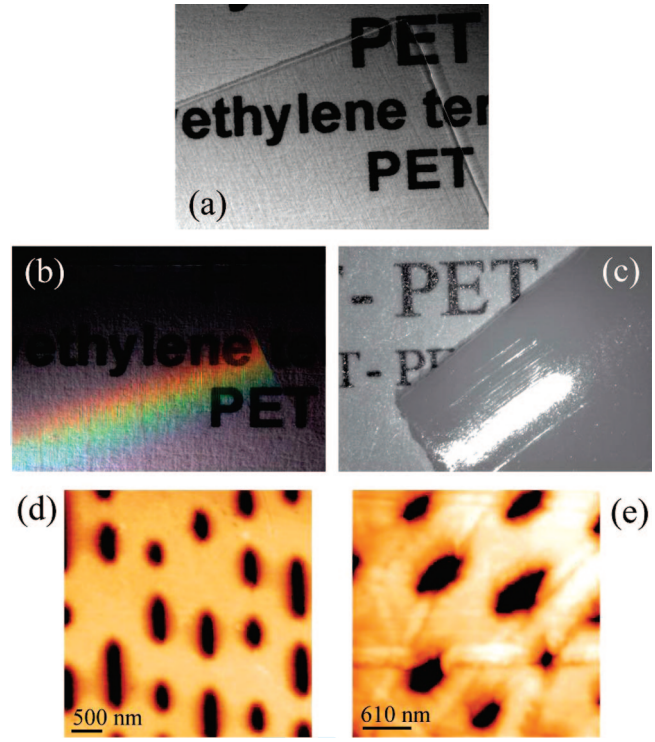

Figure 2. (a) Photograph of a BARE-PET foil on a laser printed sheet. (b) Photograph of a PET foil after imprinting at 75 °C with the "DVD"-mold (the rainbow diffraction pattern highlights the patterned area): transparency is conserved. (c) Photograph of a PET foil after imprinting at 150 °C with the "DVD"-mold: transparency is lost. (d) AFM image of PET imprinted at 75 °C with the "DVD"-mold: the pattern was successfully transferred. (e) AFM image of PET imprinted at 150 °C with the "DVD"-mold: the pattern was affected by broadening.

broadening that affected PET150. Broadened features were not present in any area of PET75, and the groove depth was comparable with the height of the pattern present on the mold. These results imply that, even at 75 °C, the polymer viscosity at the surface in contact with the mold was sufficiently reduced for successful processing. This shows that PET is suitable for HEL at unusually low temperatures. This results is quite surprising, in light of the fact that the bulk T_g of our samples would have required a much higher temperature for successful patterning. As we shall discuss in the next sections, this behavior can be addressed to a reduced T_g at the film surface.

Optical properties of PET75 were compared to those of BARE-PET by absorption analysis performed with a Jasco V-550 spectrometer. The spectra of PET75 and BARE-PET did not show significant differences in the visible range, demonstrating unaltered polymer transparency (compare optical images in Figure 2b and c).

Very high resolution nanopatterning at T_l was also demonstrated. Lines with a lateral dimension of ∼60 nm (Figure 1d) are present in our "hi-res"-molds, and this allowed testing of the technique for the replication of sub-100 nm patterns. Such dimensions constitute a relevant length scale for several applications, such as, for example, the use of nanoimprinted substrates to study cell−environment interactions[19,20] or the production of advanced electronic devices.[21] We performed HEL by using the same parameters optimized for the "DVD"-molds

(15) Zhang, Y.; Zhang, J.; Lu, Y.; Duan, Y.; Yan, S.; Shen, D. *Macromolecules* **2004**, *37*, 2532.
(16) http://www.astm.org.
(17) Liao, W.-c.; Hsu, S. L.-C.; Chu, S. Y.; Kau, P.-C. *Microelectron. Eng.* **2005**, *75*, 145.
(18) Chou, S. Y.; Krauss, P. R.; Renstrom, P. J. *Appl. Phys. Lett.* **1995**, *67*, 3114.
(19) Cecchini, M.; Bumma, G.; Serresi, M.; Beltram, F. *Nanotechnology* **2007**, *18*, 505103.
(20) Cecchini, M.; Ferrari, A.; Beltram, F. *J. Phys.: Conf. Ser.* **2008**, *100*, 012003.
(21) Yu, B.; Meyyappan, M. *Solid-State Electron.* **2006**, *50*, 536.

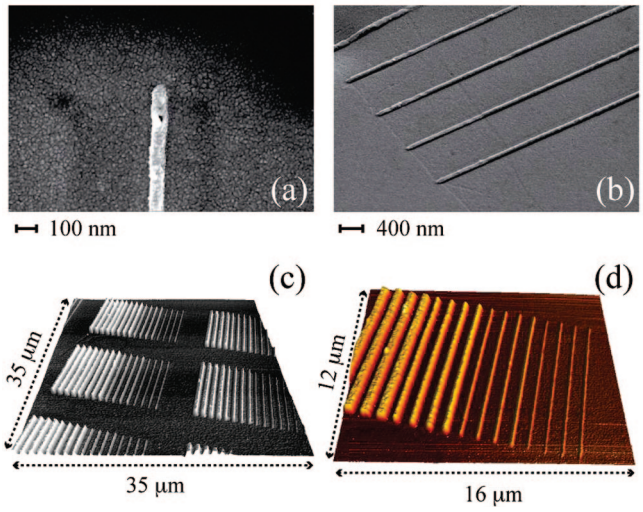

Figure 3. High-resolution PET nanoimprint lithography (75 °C, 20 bar, 300 s). (a,b) SEM images of the 75 nm wide ridges. (c,d) AFM characterization of PET nanogratings.

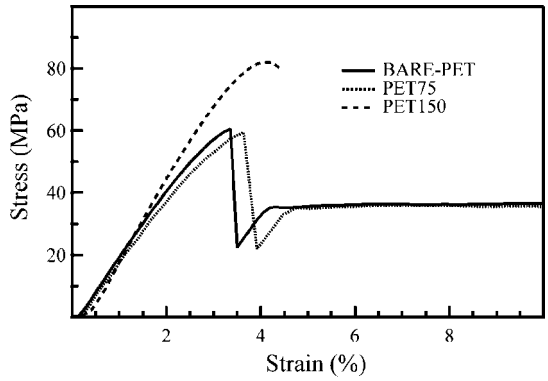

Figure 4. Typical elongation curves obtained for BARE-PET (solid line), PET150 (dashed line), and PET75 (dotted line): note the dramatic decrease in the elongation at the break of PET150 with respect to BARE-PET and PET-75.

(20 bar, t = 300 s, and T_{cool} = 50 °C). Results are summarized in Figure 3a and b, where SEM images of gold-coated imprinted substrates are reported. The patterns were properly transferred from the mold into PET75. The minimum feature size obtained was 75 nm. This broadening can be linked to polymer elastic relaxation following pressure release[22] and, presently, appears to be the dominant factor that limits process resolution. The process turned out to be very reliable and reproducible throughout the PET film, allowing sub-100 nm patterning over macroscopic areas.

Figure 3c and d displays the topography of embossed PET75 obtained by atomic force microscopy. The height of the widest ridges (i.e., 500 and 300 nm line width) was the same as the depth of the mold grooves (~80 nm). The narrowest patterns showed decreased heights, namely, 50 and 35 nm for the 150 and 75 nm line width ridges, respectively.

3.2. Tensile Tests. Tensile tests measurements were carried out in order to investigate the impact of HEL on PET bulk mechanical properties. A typical set of elongation curves used to calculate the tensile stress, strain, and elastic modulus is displayed in Figure 4, while the averaged results of the whole set of measurements are summarized in Table 1.

Table 1. Tensile Tests on PET Samples[a]

		yield		break	
entry	E-modulus (MPa)	stress (MPa)	strain (%)	stress (MPa)	strain (%)
BARE-PET	2258 ± 79	59 ± 4	3.1 ± 0.4	45 ± 5	128 ± 30
PET75	2123 ± 71	62 ± 4	3.9 ± 0.3	60 ± 10	205 ± 46
PET150	2614 ± 45	82 ± 1	4.4 ± 0.2	79 ± 2	4.7 ± 0.4

[a] Tensile stress, strain, and elastic modulus were calculated by an average of the results obtained from the load elongation curves acquired for 8−15 specimens for each sample.

The BARE-PET sample presents the typical high E-modulus, thermoplastic behavior (Table 1), showing an evident yield point and further crystallization under strain. PET150 showed very different mechanical characteristics. Indeed, we found remarkably increased stiffness, that is, higher E-modulus, and a dramatically decreased elongation at break. This was reduced down to 5% of the BARE-PET case: a severely compromised mechanical performance, especially in terms of flexibility. We link this loss of performance to a significant increase in the crystalline content as a consequence of high-temperature embossing.[23]

On the contrary, HEL at 75 °C does not affect the trend of the stress−strain curve, and very similar mechanical parameters to BARE-PET were measured for the PET75 sample. No other differences were found in tensile curves of BARE-PET and PET75 samples, demonstrating the advantage of using the "low-temperature" procedure with respect to standard high-temperature protocols.

3.3. DSC Analyses. The crystalline structure of PET is associated with a *trans* planar conformation of the terephthalate repeating unit along the chain and related to a *trans* orientation of the oxygen atoms of the glycol segment (*trans*-EG).[24] This combination displays a nearly linear chain arrangement yielding a closer packing in the crystalline regions. On the other hand, kicks induced by the *gauche* glycol and *cis*-terephthalate conformations lead to disordered nonlinear chain conformations which are formed in the amorphous phase.[24]

We performed the analysis of the bulk thermal behavior and crystallinity content of our samples by conducting DSC measurements (see section 2.3 for experimental details). The results are summarized in Table 2, while typical DSC curves obtained for the first heating scan of BARE-PET, PET150, and PET75 are shown in Figure 5. BARE-PET is characterized by a glass transition temperature of 72 °C, one large exothermic peak, centered at 142 °C (cold crystallization temperature, T_{cc}), and one endothermic peak, centered at 246 °C (melting temperature, T_m), as expected for amorphous PET samples. Indeed, the exothermic peak is due to the reorganization of amorphous domains into crystalline ones, in account of increased macromolecular freedom upon increasing temperature. The resulting crystallinity (total crystallinity) is therefore a sum of contributions, an original one and an induced one. Both crystalline phases melt together, yielding the observed endothermic peak centered at 246−250 °C. The original crystallinity enthalpy, that is, the original crystallinity content, was calculated by subtracting the cold crystallization enthalpy from the total melting enthalpy and resulted in 5% for BARE-PET.

PET150 showed neither detectable T_g nor cold crystallization, suggesting that strong modification of the film bulk structure happened owing to high-temperature HEL, although the process was carried out by contact heating (see section 2.1). The absence of the cold crystallization peak in the DSC curves (Figure 4)

(22) Scheer, H.-C.; Bogdanski, N.; Wissen, M.; Konishi, T.; HiraiScheer, Y. *J. Vac. Sci. Technol., B* **2005**, *23*, 2963.
(23) Dixon, E. R.; Jackson, J. B. *J. Mater. Sci.* **1968**, *3*, 464.
(24) Schmidt-Rohr, K.; Hu, W.; Zumbulyadis, N. *Science* **1998**, *280*, 714.

Table 2. DSC Analysis: Results from the First Heating Scan

	T_g		T_{cc}		T_m			crystallinity content	
entry	T (°C)	ΔC_p (J/g·K)	T (°C)	ΔH_{cc} (J/g)	T (°C)	ΔH_m (J/g)	$\Delta(\Delta H)$ (J/g)	total (%)	original (%)
BARE-PET	71.7	0.3	141.9	−29.3	246.2	36.3	7.0	27	5
PET75	73.4	0.3	142.9	−28.8	250.7	36.5	7.7	27	6
PET150	73.2	0.2	nd	nd	245.3	33.6	33.6	25	25

indicates an increased original crystallization content with respect to BARE-PET, that we quantified as 25%. Moreover, PET150 presented also a further endothermic peak centered at 166 °C, likely caused by the melting of crystalline domains obtained by secondary crystallization processes.[25]

On the contrary, the first heating scan of PET75 showed the same trend as that of BARE-PET, with a detectable glass transition and a strong cold crystallization exothermic peak. In particular, the transition temperatures and enthalpies of the two samples were comparable and the difference in the original bulk crystallinity content is virtually negligible (Table 2).

BARE-PET, PET150, and PET-75 presented almost identical behavior upon cooling and second heating scans, demonstrating that the induced alteration of the amorphous/crystalline ratio upon imprinting is reversible.

The low original crystallinity content at room temperature and the very similar thermal behaviors of BARE-PET and PET75 confirm that these films are mainly amorphous at room temperature and that the process carried out at 75 °C does not alter the amorphous/crystalline ratio.

3.4. ATR-FTIR Analyses. Surface crystalline content was finally studied by ATR-FTIR spectroscopy following the procedure described in section 2.4.

Figure 6 reports the full ATR-FTIR spectra obtained for BARE-PET, PET150, and PET75. The absorption region of interest is magnified in the inset, where the three peaks at 1340, 1370, and 1410 cm^{-1}, relative to the wagging vibration of CH_2 in the *trans*-EG conformer, the wagging vibration of CH_2 in the *gauche*-EG conformer,[26] and C−C stretching[27] (reference band), respectively, are fully resolved. The relative intensity of the peaks at 1340 and 1370 cm^{-1} with respect to the reference one (1410 cm^{-1}) significantly changed in sample PET150. This indicates an altered *trans*/*gauche*-EG conformer ratio. In the case of PET75, the curve was instead almost equal to that of BARE-PET, suggesting that the phase composition was quite similar in BARE-PET and PET75 samples.

Surface crystalline contents are reported in Table 3. As discussed in section 2.4, our experimental configuration allows probing surface layers with two different thickness values: 500 and 2100 nm. Samples embossed at 150 °C showed a dramatic increase in the crystalline content at the surface, evaluated up to 62% within the 0.5 μm surface thickness and around 25% within the 2.1 μm surface thickness. The surface crystallinity of PET was instead unchanged by low-temperature embossing. In fact, BARE-PET and PET75 showed the same surface crystalline content, which was found in the 8.0−9.2% range. These values are in agreement with the crystallinity content reported in the literature for amorphous PET[28] and further confirm the efficacy of the imprinting procedure at 75 °C. It is worth noting that the crystalline content evaluated by surface measurements (ATR) and by bulk analyses (DSC) is different (Table 4). As expected, the bulk analysis returned lower crystalline content with respect to surface measurements. Indeed, as described in section 2.1, the polymer was heated by contact to the heated mold, whose temperature was fixed by the imprinting machine. Owing to the low thermal conductivity of PET, this determined nonuniform heating and a temperature gradient from the sample top to the bottom surface. This is particularly evident for PET150, where surface crystallinity was estimated up to 62%, progressively

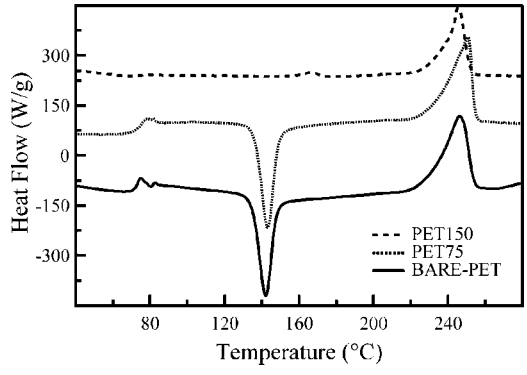

Figure 5. DSC traces from the first heating scan: heat flow as a function of the temperature for BARE-PET (solid line), PET150 (dashed line), and PET75 (dotted line).

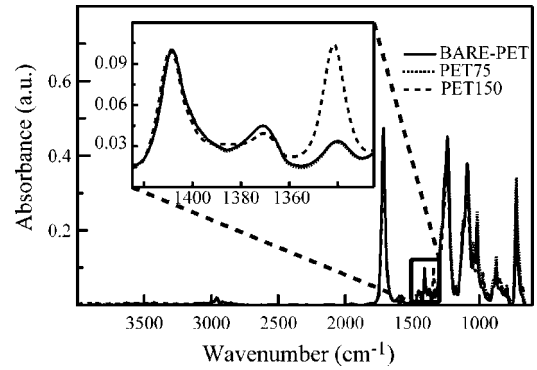

Figure 6. ATR-FTIR spectra of BARE-PET (solid line), PET75 (dotted line), and PET150 (dashed line). Inset: magnified view of the 1430−1320 cm^{-1} range. The 1340 and 1370 cm^{-1} peaks are attributed, respectively, to the *trans*-EG conformer and the *gauche*-EG conformer of the PET macromolecular chains.

Table 3. Surface Crystalline Content of PET Samples Measured by ATR-FTIR Spectroscopy[a]

	crystallinity	
	method 1 (%)	method 2 (%)
BARE-PET	8.9 ± 0.5	9.2 ± 0.5
PET75	9.0 ± 0.5	9.0 ± 0.5
PET150	62.1 ± 0.5	25.4 ± 0.5

[a] The two columns refer to different penetration depths: method 1 = 0.5 μm and method 2 = 2.1 μm.

Table 4. Comparison of the Crystalline Contents Obtained by DSC and ATR-FTIR Spectroscopy

	crystallinity		
	DSC	ATR	
	(1H) (%)	method 1 (%)	method 2 (%)
BARE-PET	5 ± 0.7	8.9 ± 0.5	9.2 ± 0.5
PET75	6 ± 0.7	9.0 ± 0.5	9.0 ± 0.5
PET150	25 ± 0.7	62.1 ± 0.5	25.4 ± 0.5

decreasing to the bulk one (25%). For what concerns BARE-PET, the difference between bulk and surface crystallinity is less pronounced and cannot be linked to the cited temperature gradient because BARE-PET was not heated at all. The presence of this increased crystallized layer at the surface was in effect also revealed by high-resolution AFM measurements (Supporting Information, Figure S1), where the surface layer appears to be rather structured. This state can be driven by a reduced T_g at the polymer surface and/or by the lamination process employed for its fabrication by the manufacturer. More in general, a decrease in T_g at the surface indicates a surface polymer chain higher mobility.[29−31] We believe that the presence of this high mobility layer at lower T_g allowed the performance of hot embossing at unusually low temperature. As reported for PET thin films and for other thermoplastic polymers, the surface T_g can indeed be significantly lower than the bulk value.[15,30,32] For the sake of examples, Ellison and Torkelson[32] measured, for polystyrene, a surface T_g more than 40 °C lower than the bulk value. Bulk T_g was progressively recovered by increasing the thickness of the measured polymer slice.

The surface crystallinity of PET75 is comparable with that of BARE-PET, demonstrating the negligible impact of "low-temperature" imprinting even to the film surface which was heated and stressed by the contact to the mold.

3. Conclusions

Low-damage nanotopographic surface modification of poly(ethylene terephthalate) (PET) was demonstrated. Nanopatterns (sub-100 nm resolution) were transferred by hot embossing lithography at unusually low temperature. We obtained reliable and high-fidelity embossing at a temperature only 3 °C greater than the T_g of PET while maintaining a low process time (300 s) and pressure (20 bar). Sample optical, mechanical, and thermal characteristics were systematically analyzed before and after embossing at low and high temperature by ATR-FTIR spectroscopy, tensile tests, and DSC. Specifically, high-temperature embossed PET turned out to be dramatically changed in terms of crystallinity content (increased from 5% to 25% and up to 62% at the surface) and mechanical behavior (increased rigidity and decreased elongation at break), and processing led to a complete transparency loss. On the contrary, our low-temperature procedure did not lead to any significant difference between embossed and bare PET properties. These results constitute a relevant advance in plastic surface processing, opening the way to the engineering of marked containers for efficient tracking and classification. Furthermore, PET is a good candidate for artificial tissues: original nanopatterned substrates are essential investigation tools for advanced bioengineering experiments.

Acknowledgment. We thank Ranieri Bizzarri for the absorption measurements and useful discussions, Antonella Manariti for help in recording ATR-FTIR spectra, and Simone Capaccioli for useful discussions. This work was supported in part by MIUR under the FIRB Project RBLA03ER38, and under the FIRB NANOPACK project 2003 D.D.2186 Prot. N. RBNE03R78E.

Supporting Information Available: AFM characterization of commercial PET foils. This material is available free of charge via the Internet at http://pubs.acs.org.

LA801706Q

(25) Chartoff, R. P. In *Thermal Characterization of Polymeric Materials*; Turi, E. A., Ed.; Academic Press: San Diego, 1997; p 616.
(26) Grime, D.; Ward, I. M. *Trans. Faraday Soc.* **1958**, *54*, 959.
(27) Liang, C. Y.; Krimm, S. J. *J. Mol. Spectrosc.* **1959**, *3*, 554.
(28) Cole, K. C.; Ajji, A.; Pellerin, E. *Macromolecules* **2002**, *35*, 770.
(29) Jones, R. A. L. *Nat. Mater.* **2003**, *2*, 645.
(30) Hyun, J.; Aspnes, D. E.; Cuomo, J. J. *Macromolecules* **2001**, *34*, 2395.
(31) de Gennes, P. G. *Eur. Phys. J. E* **2000**, *2*, 201.
(32) Ellison, C. J.; Torkelson, J. M. *Nat. Mater.* **2003**, *2*, 695.